11th World Congress on Computational Mechanics (WCCM XI)
5th European Conference on Computational Mechanics (ECCM V)
6th European Conference on Computational Fluid Dynamics (ECFD VI)
E. Oñate, J. Oliver and A. Huerta (Eds)

MODELING AND FEM ANALYSIS OF DYNAMIC PROPERTIES OF THERMALLY OPTIMAL COMPOSITE MATERIALS

MARIA NIENARTOWICZ[*] AND TOMASZ STREK[†]

[*] Institute of Applied Mechanics, Poznan University of Technology
ul. Jana Pawla II 24, 60-965 Poznan, Poland
e-mail: maria.nienartowicz@doctorate.put.poznan.pl

[†] Institute of Applied Mechanics, Poznan University of Technology
ul. Jana Pawla II 24, 60-965 Poznan, Poland
e-mail: tomasz.strek@put.poznan.pl

Key Words: *Composite materials, Optimization, Dynamic properties, FEM analysis*

Abstract. The paper is devoted to modelling and analysis of dynamic properties of modern materials. Simulations were provided for four 2D models of thermally optimal composite material. The first model was a composite with optimal topology which was obtained during numerical optimization. The next three models were laminar composites. The dynamic properties, like natural frequencies and mode shapes, were analyzed and compared for all models.

1 INTRODUCTION

The composite material is made of at least two components with different characteristics, so that it has better properties and new properties relative to the components used separately, or resulting from a simple sum of these properties. Externally, the composite is a monolithic material, but with visible boundaries between the components. There are many different types of composites, as it is presented in Fig. 1. Particle Reinforced Composites consist of particles of one or more materials and a matrix of another material that makes the material stronger. Fiber Reinforced Composites are composed of the long fiber of one material which is embedded in the matrix of the other material. Therefore, the composite is extremely strong. Sandwich Composites and Laminated Composites consist of two or more layers of different materials which are bonded together.

Properties of composites result from a few factors. The most important are the values of a certain property of each constituent material. Another significant factor is the geometrical structure of the composite, which affects the resultant value of its property. The most important of all environmental factors which influence the behaviour of composites is temperature. It is due to the fact that composites are rather sensitive to temperature and have relatively low effective thermal conductivity [1].

While creating composite materials, their dynamical properties are also worth analyzing. First, as a rule, natural natural frequencies and mode shapes are determined, which results from the

fact that these factors show how the structure will respond to dynamic load. The frequencies at which the system tends to oscillate without the absence of damping or driving force are called natural frequencies. The mode shape (normal mode of vibration) is a deformed shape of the structure which appears at a specific natural frequency of vibration. Natural frequencies and mode shapes are functions of boundary conditions and structural properties.

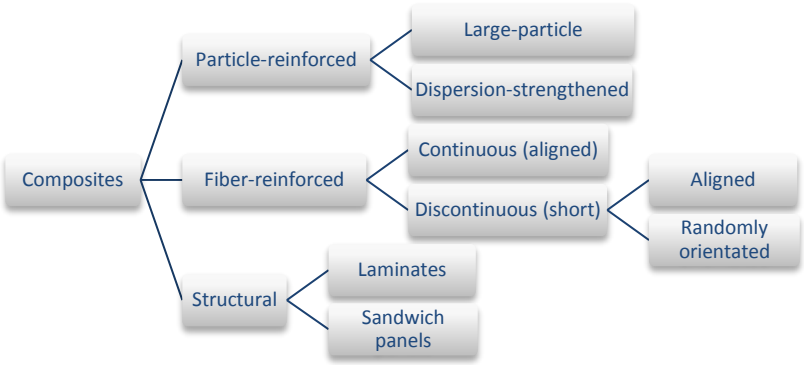

Figure 1: Composite types

In literature, one can find many examples of analysis of composite properties. A computational analysis of sandwich-structured composites with an auxetic phase is presented in [2]. Using a SIMP model, the optimal distribution of a given number of materials in a sandwich-structured composite was determined. Next, a multilayered composite structure with wavy internal layers surfaces was proposed by the authors. During calculations, the total energy strain was analyzed.

Topology optimization of the effective thermal properties of two-phase composites was performed in [3]. Calculations were made to find the optimal average temperature in a two-phase composite material. The examined composite consisted of two materials with a different value of the thermal conductivity parameter. For this purpose, different boundary conditions were applied and compared.

[4] presents research of the dynamic properties of a laminated composite magnetorheological (MR) fluid sandwich plate. The authors compared the results obtained from the present finite element formulation in terms of the natural frequencies with results accessible in the literature. To study the dynamic response of the sandwich plate under harmonic force excitations in various magnetic fields, the researchers investigated the forced vibration response of a MR fluid composite plate.

The dynamic properties of long-span steel-concrete composite bridges with external tendons were presented in [5]. For this purpose, the finite element analysis was used. During simulations, the influence of stiffness of shear connectors of composite girders, external tendons, and pile-soil dynamic interactions on the dynamic properties of steel-concrete composite bridge were taken into account.

Paper [6] presents an evaluation of mechanical properties of coconut coir fiber-reinforced polymer matrix composites. The authors described the development and characterization of a new set of natural fiber-based polyester composites consisting of coir as reinforcement and epoxy resin. Mechanical properties of the developed coir composites were evaluated for five

different volume fractions. Results of calculations and test were presented in the paper.

2 THERMALLY OPTIMAL COMPOSITE MATERIALS

A thermally optimal composite is a composite whose properties fulfill particular objective functions. Its structure can be obtained by means of optimization methods. An optimal composite is usually obtained by minimizing or maximizing the set objective function. The case of the thermally optimal composite takes thermal properties into account. Properties like average temperature, average magnitude of temperature gradient or average thermal energy can be optimized.

In the first place, to analyze the dynamic properties of a thermally optimal sandwich plate, optimization of average thermal energy was performed for the purpose of this article. The average thermal energy can be calculated by means of the formula:

$$Et_{avg} = \frac{1}{A}\int_{\Omega} Et\, d\Omega, \tag{1}$$

where Ω refers to the design domain, Et is the thermal energy and A is the area of the domain.

The considered design optimization problem depends on the design variable . Therefore, the objective function fulfills the equation:

$$Et_{avg}(r) = \frac{1}{A}\int_{\Omega} Et(r)\, d\Omega. \tag{2}$$

For the solid, the thermal energy is calculated by the following equation:

$$Et_{avg}(r) = c_p T(r), \tag{3}$$

where c_p is the heat capacity and $T(r)$ is the temperature.

Using the Fourier's law of steady state pure conduction, one can calculate the temperature:

$$-\nabla \cdot (k(r)\nabla T) = Q. \tag{4}$$

Here $k(r)$ is the thermal conductivity and Q is the heat source.

3 TOPOLOGY OPTIMIZATION USING SIMP MODEL

As it is stated above, the analysis of the dynamic properties of s thermally optimal sandwich plate was performed. To obtain such a two-phase sandwich plate, the gradient-based algorithm SNOPT for a large-scale optimization was used. The Sparse Nonlinear OPTimizer code was developed by Gill, Murray and Saunders [7]. The algorithm allows to apply any form of the objective function and any constraints. It is used for the constrained optimization, which minimizes a linear or nonlinear function subject to bounds on the variables and sparse linear or nonlinear constraints. SNOPT finds locally optimal solutions using the sequential quadratic programming (SQP) algorithm.

For the purpose of a topology optimization, a model of solid isotropic material with penalization (SIMP) was used. It is an interpolation model for the material properties [8]. SIMP is used in optimal topology, where structure should consist solely of a macroscopic variation of one material and void, which means that the density of the structure is given by a "0-1" integer

parameterization (black-and-white design). Using a SIMP model in topology optimization of a two-phase sandwich plate, the thermal conductivity can be written in the form of:

$$k(r) = k_1 + (k_2 - k_1) \cdot r^p, \qquad p > 1, \qquad k_1 < k_2, \tag{5}$$

where r is a control variable (design variable), p is a penalty parameter, k_1 and k_2 are thermal conductivity values of the first and the second material respectively.

The control variable, which is related to thermal conductivity parameter for isotropic material, is interpolated from 0 (for the first material) to 1 (for the second material). The penalty parameter affects the material distribution. When its value is above 1, the density values 0 or 1 are favoured ahead of the intermediate values.

In the presented calculations, the design variable was interpreted as generalized material density, which fulfills the formula (6). Assigning each element an individual control variable value, the optimal material distribution was found, taking into account the objective function and constraints.

$$0 \le \int_\Omega r(x)\, d\Omega \le V, \quad 0 \le r(x) \le 1. \tag{6}$$

To obtain the distribution of the control variable, an optimization was performed for a 2D model with boundary condition applieds as it is shown in Figure 1. The first material was polyurethane foam and the second material, whose fraction of distribution A_{frac}=0.4, was steel. The values of properties for both materials are compared in Table 1. Minimizing thermal energy, the distribution of the control variable took form as presented in Figure 2. Value 1 (red colour) indicates steel, and value 0 (blue colour) indicates polyurethane foam.

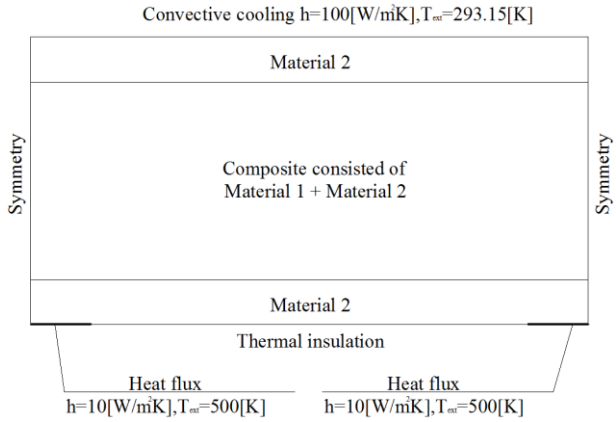

Figure 1: Boundary conditions

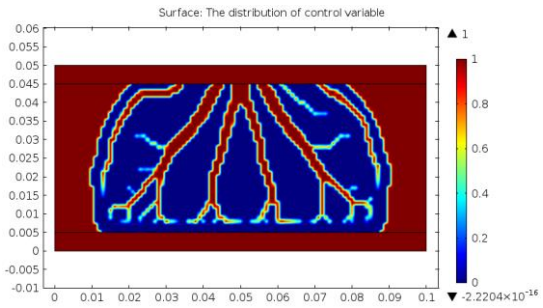

Figure 2: The distribution of control variable

Table 1: Values of thermal and mechanical properties of the model

Property	Polyurethane foam Material 1	Steel Material 2
k [W/mK]	0.03	58
ρ [kg/m^3]	50	8000
ν	0.4	0.25
E [Pa]	4e9	2e11

The value of the minimized average thermal energy in the sandwich plate was compared with values for three types of laminate composites (first with a steel layer in the middle, second with a steel layer at the bottom, and the third with a steel layer on top), as shown in Figures 3 - 5. The values of average thermal energy are presented in Table 1.

Table 2: Values of average thermal energy

Material type	Values of average thermal energy [m^2/s^2]
Sandwich plate	1.4129e5
Laminate 1	1.69958e5
Laminate 2	1.79572e5
Laminate 3	1.6038e5

As it can be seen, the smallest value of average thermal energy was obtained for the thermally optimal sandwich plate. The biggest value appeared in the second laminate, where the steel layer was close to thermal insulation.

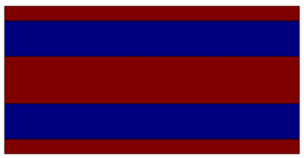

Figure 3: Laminate 1 - steel layer in the middle

Figure 4: Laminate 2 - steel layer at the bottom

Figure 5: Laminate 3 - steel layer at the top

For the purpose of the analysis of dynamic properties, Young's modulus, Poisson's ratio and density can be also written using a SIMP model:

$$\rho(r) = \rho_1 + (\rho_2 - \rho_1) \cdot r^p, \qquad p > 1\,, \quad \rho_1 < \rho_2 \tag{7}$$

$$\nu(r) = \nu_1 + (\nu_2 - \nu_1) \cdot r^p, \qquad p > 1\,, \quad \nu_1 > \nu_2 \tag{8}$$

$$E(r) = E_1 + (E_2 - E_1) \cdot r^p, \qquad p > 1\,, \quad E_1 < E_2 \tag{9}$$

where: ρ_1 and ρ_2 are densities, ν_1 and ν_2 are Poisson's ratios, E_1 and E_2 are Young's moduli, for the first and the second material respectively.

4 ANALYSIS OF DYNAMIC PROPERTIES

Having the thermally optimal sandwich plate, the dynamic properties like natural frequencies and mode shapes can be analyzed. Simulations were provided for four 2D models, one of which was a thermally optimal sandwich plate, and the remaining three were laminates, all presented in Figures 3 – 5. For all of them, boundary conditions, presented below in Figure 6, were applied. The boundary load fulfills the formula:

$$F(t) = F_l \sin(\omega t), \text{ where } F_l = 10000\ [N/m^2]. \tag{10}$$

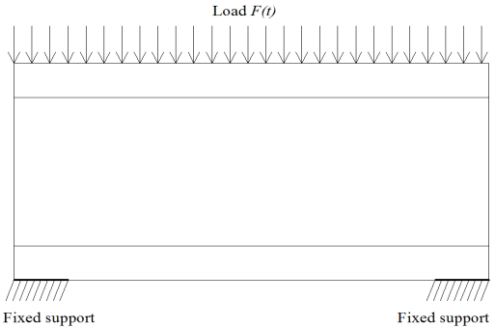

Figure 6: Boundary conditions for dynamic properties analysis

For the linear constitutive relation between stresses and deformations, the calculations used the Navier's equation of motion for isotropic solid [9]:

$$\rho \frac{\partial^2 \boldsymbol{u}}{\partial t^2} - (\mu \nabla^2 \boldsymbol{u} + (\lambda + \mu) \nabla \nabla \cdot \boldsymbol{u}) = \boldsymbol{0}. \tag{11}$$

For each model, six eigenfrequencies were determined. The values are presented in Table 2.

Table 3: Values of eigenfrequencies

No.	1	2	3	4	5	6
Value of eigenfrequencies for sandwich plate [Hz]	5502.93	7712.40	14618.93	15047.05	17713.10	19548.60
Value of eigenfrequencies for laminate 1 [Hz]	3606.20	4482.82	7123.74	10376.22	11651.42	13137.66
Value of eigenfrequencies for laminate 2 [Hz]	5468.04	8546.50	12111.30	12925.40	15020.60	15375.50
Value of eigenfrequencies for laminate 3 [Hz]	2593.97	3718.00	5764.30	11591.82	15148.03	16681.87

Figures 7 – 12 present the amplitudes of the forced vibration and mode shapes for each eigenfrequency for the sandwich plate.

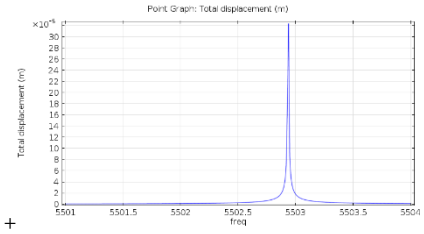

Figure 7: a) The amplitude of forced vibration in sandwich plate

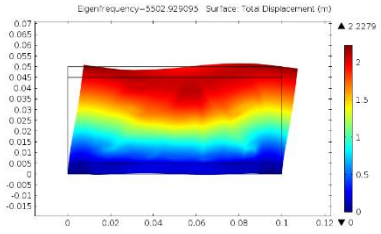

Figure 7: b) Mode shape for the first eigenvalue in sandwich plate

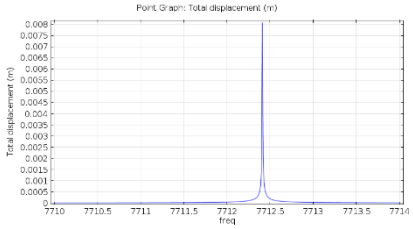

Figure 8: a) The amplitude of forced vibration in sandwich plate

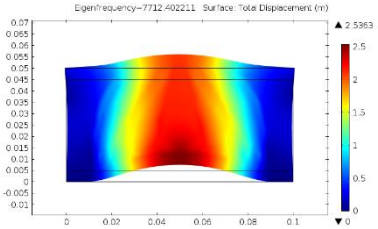

Figure 8: b) Mode shape for the second eigenvalue in sandwich plate

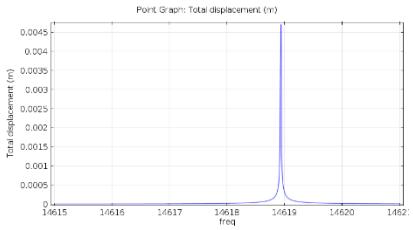

Figure 9: a) The amplitude of forced vibration in sandwich plate

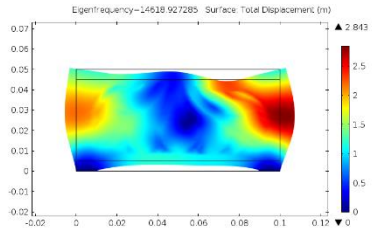

Figure 9: b) Mode shape for the third eigenvalue in sandwich plate

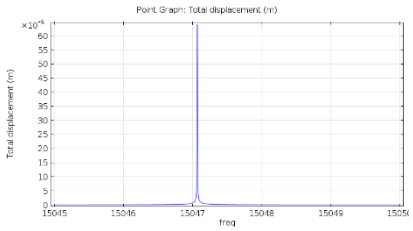

Figure 10: a) The amplitude of forced vibration in sandwich plate

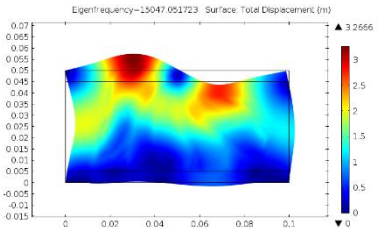

Figure 10: b) Mode shape for the fourth eigenvalue in sandwich plate

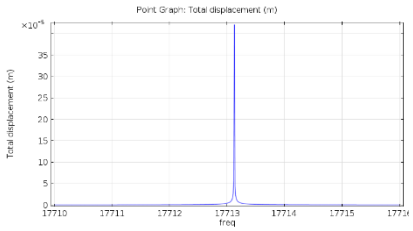

Figure 11: a) The amplitude of forced vibration in sandwich plate

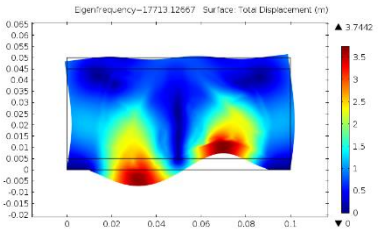

Figure 11: b) Mode shape for the fifth eigenvalue in sandwich plate

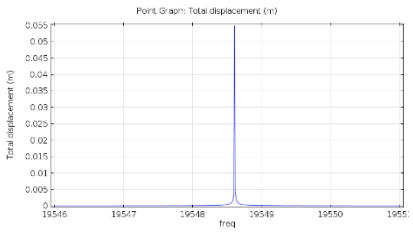

Figure 12: a) The amplitude of forced vibration in sandwich plate

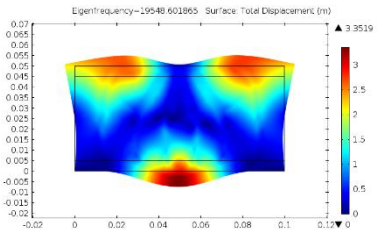

Figure 12: b) Mode shape for the sixth eigenvalue in sandwich plate

Figures 13 - 18 present the amplitudes of the forced vibration and mode shapes for each eigenfrequency for laminate 1.

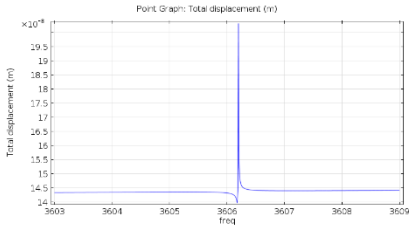

Figure 13: a) The amplitude of forced vibration in laminate 1

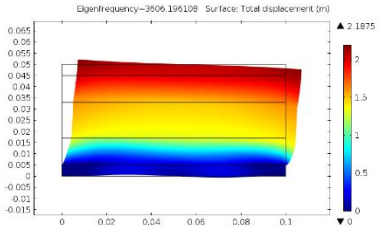

Figure 13: b) Mode shape for the first eigenvalue in laminate 1

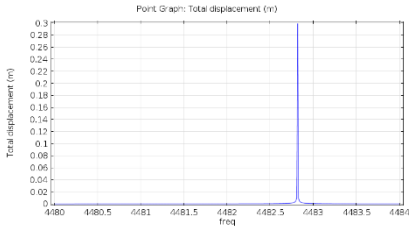

Figure 14: a) The amplitude of forced vibration in laminate 1

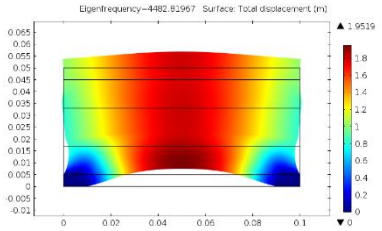

Figure 14: b) Mode shape for the second eigenvalue in laminate 1

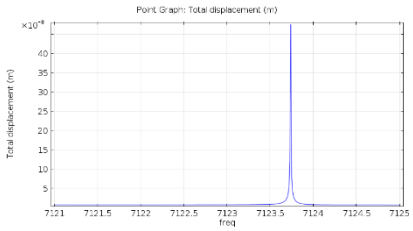

Figure 15: a) The amplitude of forced vibration in laminate 1

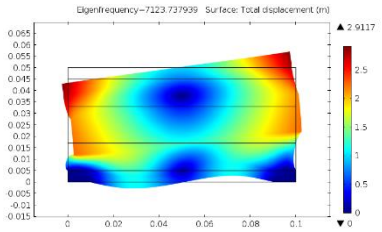

Figure 15: b) Mode shape for the third eigenvalue in laminate 1

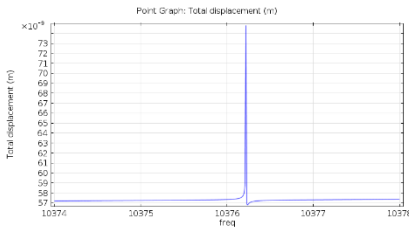

Figure 16: a) The amplitude of forced vibration in laminate 1

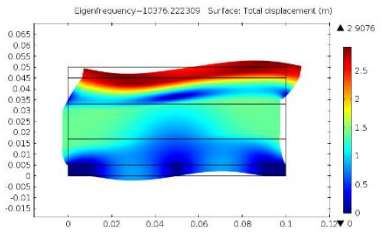

Figure 16: b) Mode shape for the fourth eigenvalue in laminate 1

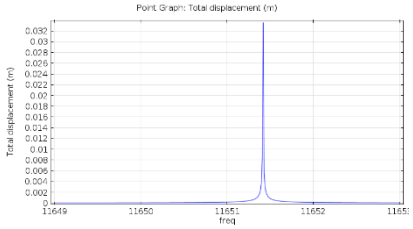

Figure 17: a) The amplitude of forced vibration in laminate 1

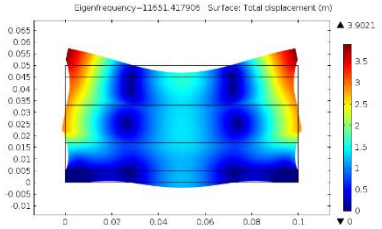

Figure 17: b) Mode shape for the fifth eigenvalue in laminate 1

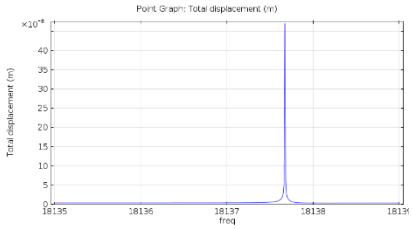

Figure 18: a) The amplitude of forced vibration in laminate 1

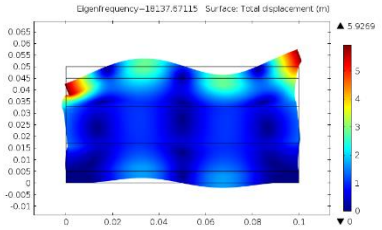

Figure 18: b) Mode shape for the sixth eigenvalue in laminate 1

Figures 19 - 24 present the amplitudes of the forced vibration and mode shapes for each eigenfrequency for laminate 2.

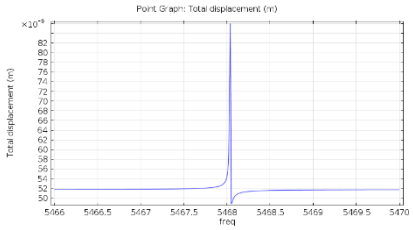

Figure 19: a) The amplitude of forced vibration in laminate 2

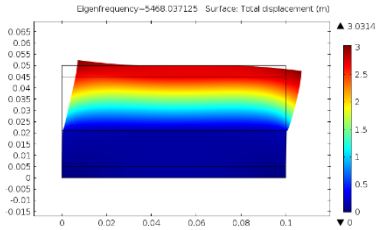

Figure 19: b) Mode shape for the first eigenvalue in laminate 2

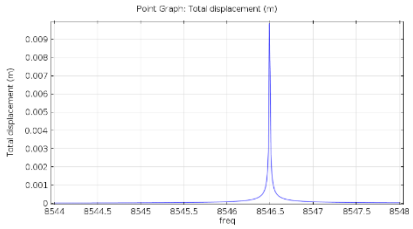

Figure 20: a) The amplitude of forced vibration in laminate 2

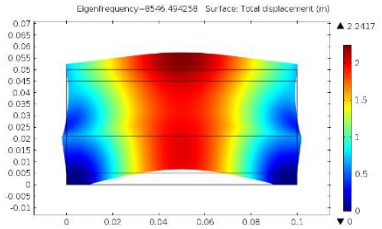

Figure 20: b) Mode shape for the second eigenvalue in laminate 2

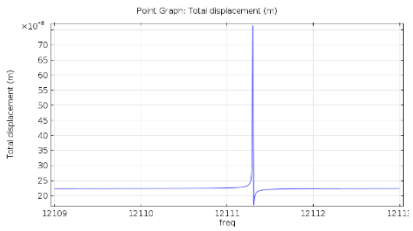

Figure 21: a) The amplitude of forced vibration in laminate 2

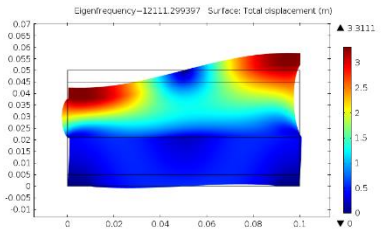

Figure 21: b) Mode shape for the third eigenvalue in laminate 2

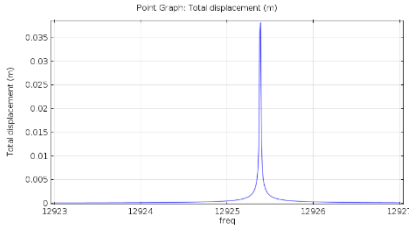

Figure 22: a) The amplitude of forced vibration in laminate 2

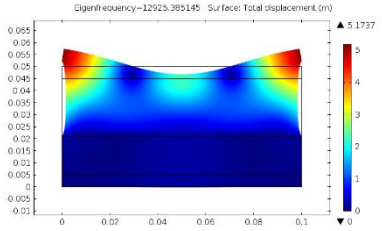

Figure 22: b) Mode shape for the fourth eigenvalue in laminate 2

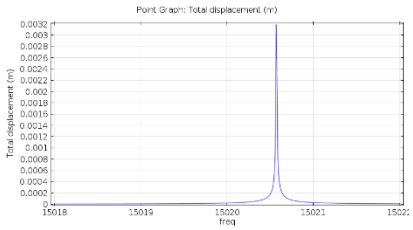

Figure 23: a) The amplitude of forced vibration in laminate 2

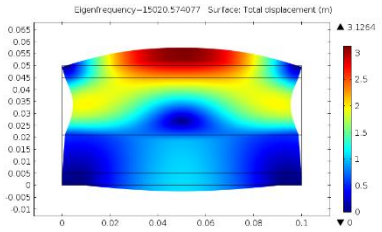

Figure 23: b) Mode shape for the fifth eigenvalue in laminate 2

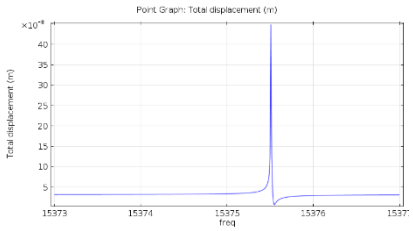

Figure 24: a) The amplitude of forced vibration in laminate 2

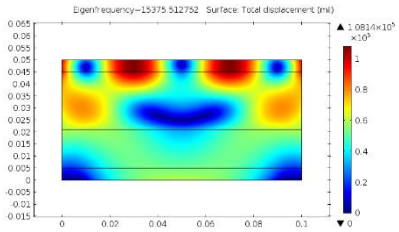

Figure 24: b) Mode shape for the sixth eigenvalue in laminate 2

Figures present 25 - 30 the amplitudes of the forced vibration and mode shapes for each eigenfrequency for laminate 3.

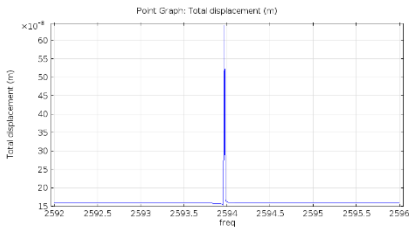

Figure 25: a) The amplitude of forced vibration in laminate 3

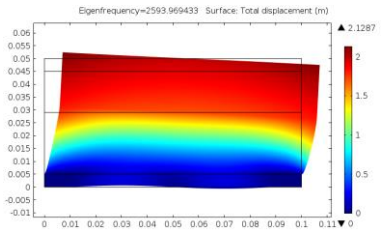

Figure 25: b) Mode shape for the first eigenvalue in laminate 3

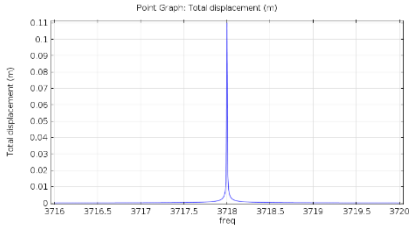

Figure 26: a) The amplitude of forced vibration in laminate 3

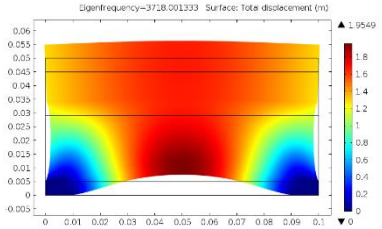

Figure 26: b) Mode shape for the second eigenvalue in laminate 3

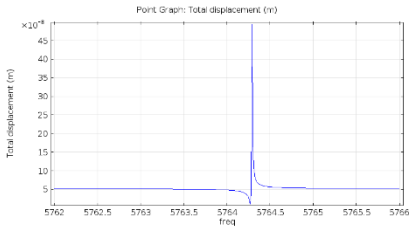

Figure 27: a) The amplitude of forced vibration in laminate 3

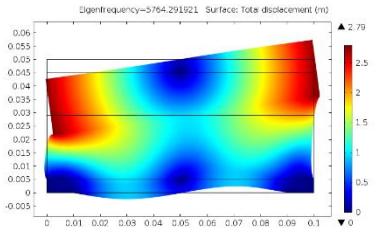

Figure 27: b) Mode shape for the third eigenvalue in laminate 3

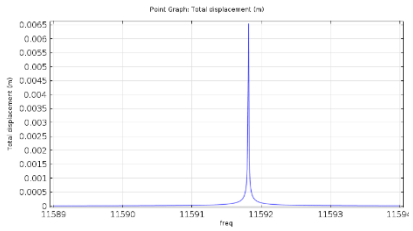

Figure 28: a) The amplitude of forced vibration in laminate 3

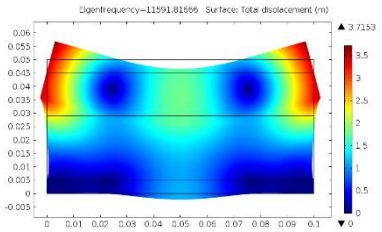

Figure 28: b) Mode shape for the fourth eigenvalue in laminate 3

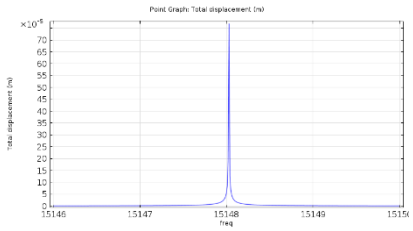

Figure 29: a) The amplitude of forced vibration in laminate 3

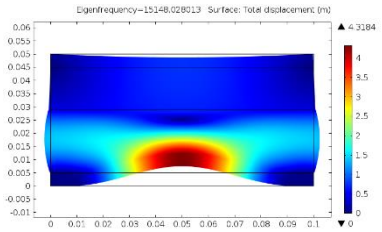

Figure 29: b) Mode shape for the fifth eigenvalue in laminate 3

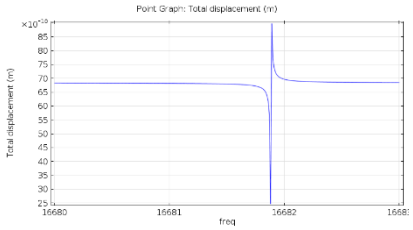

Figure 30: a) The amplitude of forced vibration in laminate 3

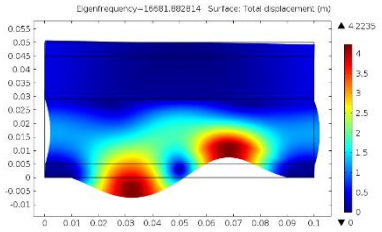

Figure 30: b) Mode shape for the sixth eigenvalue in laminate 3

12 CONCLUSIONS

The paper presents the analysis of dynamic properties like eigenfrequencies and mode shapes of composite structures. Simulations were provided for a thermally optimal sandwich plate and three types of laminates. Minimization of average thermal energy showed that the smallest value of average thermal energy can be obtained for the proposed sandwich panel. For each model, six eigenfrequencies were determined. Next, the amplitudes of forced vibration and mode shapes for each model were presented.

ACKNOWLEDGEMENTS

This research was supported by the International Association for Computational Mechanics (IACM) and by the MNiSW grants 02/21/DSMK/0429.

REFERENCES

[1] Jopek H. and Strek T. Optimization of the Effective Thermal Conductivity of a Composite, *Convection and Conduction Heat Transfer*, Amimul Ahsan (Ed.), InTech (2011).

[2] Strek T., Jopek H., Maruszewski B. T., Nienartowicz M., Computational analysis of sandwich-structured composites with an auxetic phase, *Phys. Status Solidi (b)*, (2014) Vol. 251, Issue 2: 354-366.

[3] Nienartowicz M., Strek T., Topology optimization of the effective thermal properties of two-phase composites, *Recent Advances in Computational Mechanics*, T. Łodygowski, J. Rakowski, P. Litewka (Ed.), CRC Press, (2014).

[4] Manoharan R, Vasudevan R and Jeevanantham A K., Dynamic characterization of a laminated composite magnetorheological fluid sandwich plate, *Smart Mater. Struct.* (2014) **23**: 025022.

[5] Wang W.A. , Li Q. , Zhao C.H. , Zhuang, W.L. , Dynamic properties of long-span steel-concrete composite bridges with external tendons, *Advanced Materials Research*, (2014) **831**: 359-363.

[6] Naveen, P.N.E. , Dharma Raju, T. , Evaluation of mechanical properties of coconut coir fiber reinforced polymer matrix composites, *Journal of Nano Research* (2013) **24**: 34-45.

[7] Gill P.E., Murray W. and Saunders M.A., SNOPT: An SQP Algorithm for Large-Scale Constrained Optimization, *SIAM REVIEW* (2005) **47**: 99–131.

[8] Bendsoe M. P., Sigmund O., Material interpolation schemes in topology optimization, *Archive of Applied Mechanics* (1999) **69**: 635-654.

[9] Lautrup B., *Physics of Continuous Matter, Exotic and Everyday Phenomena in the Macroscopic World*, IOP, (2005).